International Journal of Sciences: Basic and Applied Research (IJSBAR)

ISSN 2307-4531
(Print & Online)

http://gssrr.org/index.php?journal=JournalOfBasicAndApplied

A Conceptual Abstraction for Human-Computer Interaction: Data Notes for the Development of New Techniques for Magnetic Resonance Imaging

Hugues Gentillon[a*], Ludomir Stefańczyk[b], Michał Strzelecki[c], Maria Respondek-Liberska[d]

[a]*Department of Radiology and Diagnostic Imaging, Barlicki University Hospital, Medical University of Łódź*

[a,b,c]*Institute of Electronics, The Faculty of Electrical, Electronic, Computer and Control Engineering, Technical University of Łódź, Poland*

[d]*Diagnosis and Prevention of Congenital Malformations, Instytut Centrum Zdrowia Matki Polki, Łódź, Pola*

Abstract

In applied artificial intelligence, abstraction is a conceptual process by which complex systems are simplified, for the sake of improving human-computer interaction. This manuscript presents MaZda 5 RC, a software framework for magnetic resonance imaging (MRI). Though its intended application is MRI, this abstraction system can be used in any area of research and professional practice — especially wherever high-dynamic range (HDR) still and motion media need to be analyzed with computer vision. In this data descriptor, a set of techniques was introduced to investigate the visually-lossless aspects of different image acquisition formats. 1.5/3T DICOM files were decoded to RAW images (sRGB-48) for investigation of noise and artifacts. Additional techniques were used to quantify and visualize the invisible effects of noise and artifacts in magnetic resonance (MR) images of two human fetuses.

---

*Corresponding author.

Algorithmic sorting was used to reduce more than 300 computerized values to 13 epitomic parameters (i.e. a numerical representation of the difference between the original and the denoised images). The 13 epitomic parameters were subsequently used to investigate bit-depth and artifacts in uncompressed HDR images of prenatal brain originally captured with 1.5/3T MRI scanners. As hypothesized, no qualitative difference was observed when LCD monitors were set to "pass-thru mode" (i.e. not rendered). On the other hand, MaZda was however able to quantitatively visualize a difference. Corresponding software is available at doi: 10.17632/dkxyrzwpzs.1

Keywords: imaging technology; 3d; algorithms; magnetic resonance; fetal brain; computer-assisted radiology; hugues gentillon; Mazda; b11; cybernetics; applied artificial intelligence; hci; medicine.

1. Introduction

In the medical profession, general practitioners, as well as specialists and physician-scientists, are trained to think mechanically and relevantly — i.e. effectively and efficiently, in terms of anamnesis and differential diagnosis to treat and cure patients but as well as to balance risks and benefits, and as prudently as possible. Learning the craft of medicine requires continuing training, evidence-based practice and research [1,2]. Medicine is not just about knowing the theory, technicality, regional system and bureaucratic administration. It also factors in applied critical thinking, continuing training and development. Strategic therapy must make sense, be feasibly practical in appropriate medical settings, correlate with the patient's environment, alleviate the symptoms and be altered in case of treatment or failure [3,4]. In addition, clinicians have to also deal with beneficence versus maleficence (nonfeasance, misfeasance, malfeasance), written informed consent and confidentiality, as well as malpractice versus lawsuits [3,4,5]. With increasing societal complexities, responsibilities and psychological stressors, medical doctors, especially radiologists, are coming under escalating pressure to be imaging experts and change conventional remedies with "sorcerer's apprenticeship" — i.e. training in multidisciplinary fields such as imaging science, computer science, applied artificial intelligence — and practicing medicine with perfectionated emulators of the human visual system, in order to narrow their margin of error [6,7]. Imaging technology is a defensive medicine for 21st century medical specialists, even for dermatologists [8]. Sophisticated tools are rapidly and constantly transforming radiology from a mere medical service to an advanced discipline, focused on front-line research of visualizing the future of medicine and seeking solutions for tomorrow's clinical issues, by working ahead of ordinary ailments and iatrogeneses (e.g., but not limited to, adverse effects and medical errors) — so that the unforeseen complications are truly inevitable and perceived as real aberrations rather than norm-constrained neglects [9,10,11].

2. Methods

This primary study was approved by the Research Ethics Committee at the Medical University of Łódź (MUL). Its aim was to use MaZda package version 5 to assess the effects of noise and artifacts in fetal brain images captured with 1.5/3T MRI scanners. Written- informed consent was obtained from sample donors at MUL hospitals. Two MR samples were collected from two different patients (ethical application reference

#: RNN/213/13/KE).

2.1. About the software

In 1996, the medical electronics department at the Technical University of Łódź (TUL) conceived and designed a software framework called MaZda (open source C++ library) [12,13]. In 1998, it was further developed and customized to fit the need of researchers working on the B11 project, an international research financed by the European Commission and Cooperation in Science and Technology (COST). The main objective of the B11 project was to develop quantitative methods for magnetic resonance imaging (MRI) [12,13]. The B11 module can be run within MaZda or as a standalone software. Over the years, additional modules were incorporated in MaZda. In this brief communication, we reported the latest nightly built MaZda package (version 5 RC: doi: 10.17632/dkxyrzwpzs.1). Geometry modules were added, and feature mapping is more functional. Links to related materials and datasets are provided in the online methods and references sections.

Texture analysis with MaZda was very sensitive, but our clinically-trained experts were able to repeat it. The various counter-claims documented in the literature in favor of automatic segmentation are questionable, still-emerging and perhaps fallaciously overstated [14]. Such algorithms have been tested in controlled environment. Clinical trials need to be conducted in various practical settings. To this date, we are almost certain that algorithms for automatic segmentation of developing fetal brain have not been rigorously tested in evidence-based practice.

They could complement, but they could not replace the brain of a medical expert in all facets of medicine [14]. For example, they could be utilized as complementary tools by neurosurgeons performing real-time, MRI-guided, minimally invasive brain surgery, manually or robotically. Automatic segmentation of newborn brain MRI has been theoretically claimed in the literature. The findings are limited and have been obtained in controlled settings [14]. In real life environment, interaction of expert clinicians is still needed for confirmation of final diagnostic decision.

2.2. Data collection

Over 300 parameters were calculated from image histogram, gradient, run-length matrix (RLM), co-occurrence matrix (COM), autoregressive model (AR), wavelet transform, geometry (see appendix). MaZda version 4.6 and B11 version 3.3 are available through an open-source license for use in any type of studies (http://www.eletel.p.Łódź.pl/programy/ mazda/index.php?action=mazda 46). MaZda version 4.6 was further upgraded to version 5 RC by TUL. MaZda is a freely available software system built in C++ library. Package version 5 RC, its latest nightly build, was developed and made available (doi: 10.17632/dkxyrzwpzs.1).

Figure 1 presents a schematic overview of the research. Figure 2 shows how preprocessing and classification were carried out in MaZda. The steps to view RAW image are illustrated in figure 3.

A schematic overview showing a method to visualize the difference due to de-noising and removal of artifacts

in 1.5/3T magnetic resonance images. **A.** Hundreds of parameters were extracted with MaZda version 5 RC. **B.** Computer vision was used to simplify and speed up the process (algorithms in MaZda). **C/D.** Images created with three-dimensional (3D) mesh rendering in Photoshop CS6 64-bit Extended.

E/F. Still and motion media created with 3D space module in MaZda (for video files, see raw data: DOI: 10.13140/RG.2.1.3252.1842). **G/H/I/J.** 2D-epitomic maps generated in MaZda were rendered to 3D images in Photoshop, in order to further examine the difference due to removal of noise and artifacts in the images (rotatable 3D images provided in supplemental data).

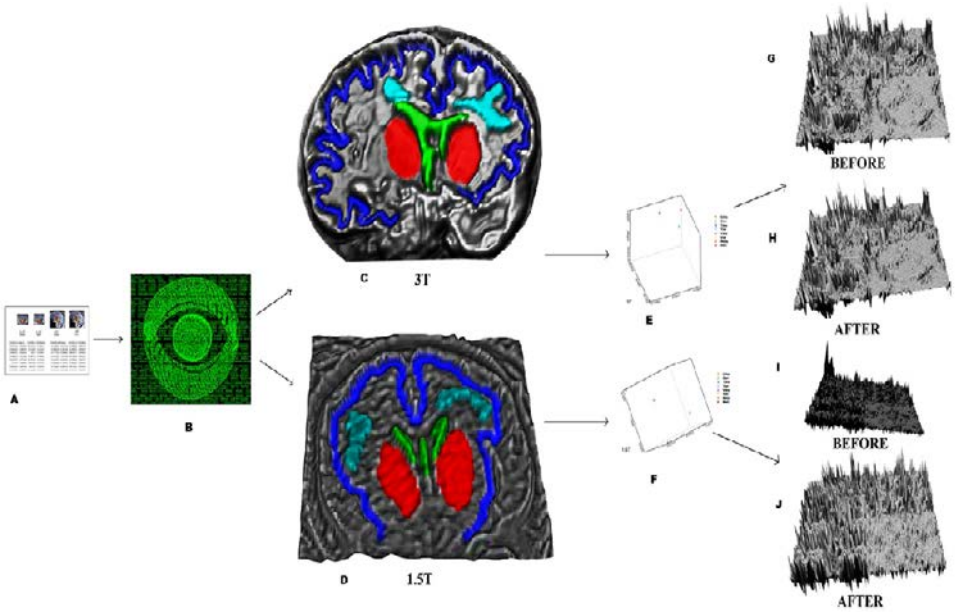

Figure 1: Computer vision

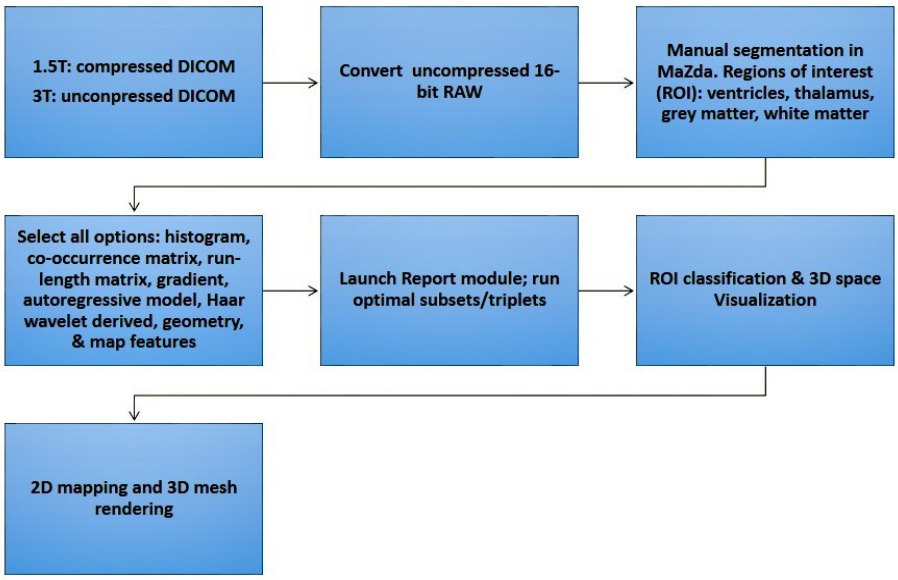

Figure 2: Schematic overview of the processing steps

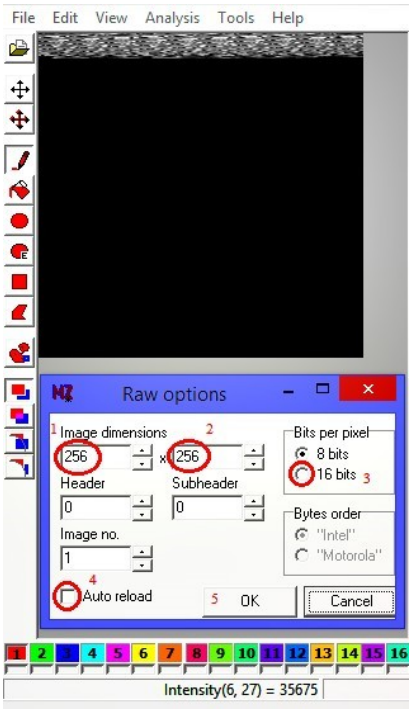

Figure 3: For RAW files, image dimension must be manually entered

MaZda was used to extract 13 epitomic parameters for 2D/3D texture visualization of regions of interest (ROI) in magnetic resonance (MR) images (table 1 and 2).

Table 1: Extraction of representative parameters in 1.5T MR images

CATEGORY	ATETA4	ATETA3	ATETA2	ATETA1	CH1D8DIF	CH1D8DIF
VORI	0.059167	0.512782	-0.08935	0.467384	1.205187	47.20759
TORI	0.360163	0.186282	-0.4412	0.671392	1.358207	82.34776
GORI	0.303222	-0.10195	0.189376	0.775859	1.491212	94.67022
WORI	0.426983	0.054579	0.217425	0.303658	1.057069	13.69683
VDNS	0.053742	0.543602	-0.11235	0.473585	1.192456	46.9687
TDNS	0.364116	0.183026	-0.44167	0.675988	1.276414	82.94204
GDNS	0.303118	-0.10201	0.18946	0.777288	1.483452	94.64518
WDNS	0.416114	0.088983	0.202644	0.302528	1.049569	12.86465

Quantification of ATETA4, ATETA3, ATETA2, ATETA1, CH1D8DIF, and CH1D8DIF: 13 epitomic parameters were extracted from 1.5T MR images using ANN algorithms in MaZda. | table 1 and 2 show values of 12 parameters, except wavelet. Representation of the wavelet was built from WavEnHL_s-3, WavEnLH_s-3, WavEnLL_s-3, WavEnHH_s-2, WavEnHL_s-2, WavEnLH_s-2, WavEnLL_s-2, WavEnHH_s-1, and WavEnHL_s-1. Details about wavelet values are available in the raw datasets: DOI: 10.13140/RG.2.1.3252.1842. Abbreviations: ORI = original; DNS = denoised; V = ventricles; T = thalamic nuclei; G =

Table 2: Extraction of representative parameters in 1.5T MR images

CATEGORY	CH1D8ENT	CH1D8INV	CH1D8COR	ASIGMA	CH1D8CON	CH1D8ANG
VORI	2.559051	0.155957	0.531011	0.493465	88.39159	0.003273
TORI	1.827896	0.097477	0.369233	0.540975	257.3429	0.015102
GORI	2.635152	0.065705	0.426331	0.829263	261.7	0.002472
WORI	2.185596	0.20363	0.744613	0.522798	33.08772	0.008041
VDNS	2.548831	0.178232	0.538674	0.475384	84.45955	0.003304
TDNS	1.827896	0.106075	0.3717	0.540093	256.4286	0.015102
GDNS	2.635447	0.061852	0.426115	0.828796	260.952	0.002432
WDNS	2.175681	0.210616	0.755589	0.496569	31.11404	0.007849

Quantification of CH1D8ENT, CH1D8INV, CH1D8COR, ASIGMA, CH1D8CON, CH1D8ANG, except WAVELET**:** 13 epitomic parameters were extracted from 1.5T MR images using ANN algorithms in MaZda. | table 1 and 2 show values of 12 parameters, except wavelet. Representation of the wavelet was built from WavEnHL_s-3, WavEnLH_s-3, WavEnLL_s-3, WavEnHH_s-2, WavEnHL_s-2, WavEnLH_s-2, WavEnLL_s-2, WavEnHH_s-1, and WavEnHL_s-1. Details about wavelet values are available in the raw datasets: DOI: 10.13140/RG.2.1.3252.1842. Abbreviations: ORI = original; DNS = denoised; V = ventricles; T

Table 3: Extraction of representative parameters in 3T MR images

CATEGORY	ATETA4	ATETA3	ATETA2	ATETA1	CH1D8DIF	CH1D8DIF
VORI	3.11E-15	0.201117	0.798883	-1.97E-15	0.29432	1.370151
TORI	0.010351	0.80445	-0.55666	0.749835	1.011794	9.064993
GORI	0.271632	0.744251	-0.3076	0.396416	1.476675	241.4201
WORI	-0.2171	1.105977	-0.68539	0.818795	1.090319	14.71334
VDNS	-0.0014	0.17694	0.830239	-0.00384	0.29432	1.370151
TDNS	0.005001	0.826408	-0.58478	0.761085	1.001065	8.850671
GDNS	0.27209	0.744815	-0.30791	0.396246	1.470401	240.7123
WDNS	-0.21874	1.111412	-0.69144	0.822774	1.07084	14.50776

Quantification of ATETA4, ATETA3, ATETA2, ATETA1, CH1D8DIF, and CH1D8DIF: 13 epitomic parameters were extracted from 3T MR images using ANN algorithms in MaZda. | table 3 and 4 show values of 12 parameters, except wavelet. Representation of the wavelet was built from WavEnHL_s-3, WavEnLH_s-3, WavEnLL_s-3, WavEnHH_s-2, WavEnHL_s-2, WavEnLH_s-2, WavEnLL_s-2, WavEnHH_s-1, and WavEnHL_s-1. Details about wavelet values are available in the raw datasets: DOI: 10.13140/RG.2.1.3252.1842. Abbreviations: ORI = original; DNS = denoised; V = ventricles; T = thalamic nuclei; G = grey matter; W = white matter).

Table 4: Extraction of representative parameters in 3T MR images

CATEGORY	CH1D8ENT	CH1D8INV	CH1D8COR	ASIGMA	CH1D8CON	CH1D8ANG
VORI	0.397905	0.879124	0.153401	1.11E-15	1.538462	0.638725
TORI	2.571508	0.235824	0.948026	0.181194	22.96755	0.003207
GORI	2.755589	0.113251	0.777761	0.385403	396.4077	0.001918
WORI	2.343412	0.174849	0.832505	0.27259	38.19429	0.005551
VDNS	0.397905	0.879124	0.153401	0.003583	1.538462	0.638725
TDNS	2.580987	0.247901	0.950069	0.173411	21.90856	0.003246
GDNS	2.748291	0.11424	0.778281	0.384713	394.7381	0.001931
WDNS	2.346636	0.172285	0.835431	0.267649	37.27429	0.005355

Quantification of CH1D8ENT, CH1D8INV, CH1D8COR, ASIGMA, CH1D8CON, CH1D8ANG, except WAVELET: 13 epitomic parameters were extracted from 3T MR images using ANN algorithms in MaZda. | table 3 and 4 show values of 12 parameters, except wavelet. Representation of the wavelet was built from WavEnHL_s-3, WavEnLH_s-3, WavEnLL_s-3, WavEnHH_s-2, WavEnHL_s-2, WavEnLH_s-2, WavEnLL_s-2, WavEnHH_s-1, and WavEnHL_s-1. Details about wavelet values are available in the raw datasets: DOI: 10.13140/RG.2.1.3252.1842. Abbreviations: ORI = original; DNS = denoised; V = ventricles; T = thalamic nuclei; G = grey matter; W = white matter).

Noise-reduction plugin in Photoshop CS6 64-bit Extended was used to remove artifact in 1.5/3- tesla (T) samples. Manual segmentation of ROIs was performed. To demonstrate the importance of image acquisition, CGI was used to create a vector image, which was then converted to various pixelated formats (sRGB-24, sRGB-32, sRGB-48, sRGB-64, sRGB-96, sRGB-128).

The purpose of this preliminary investigation was to try to humanly perceive the difference between HDR formats (figure 4, 5). For example, it was not possible to notice a difference when sRGB-24 and sRGB-48 images are viewed in software viewer like Microsoft Paint. Image rendering was used to observe the difference.

A vector image was created by conglomerating all the parameters extracted from the MR images. The collage was exported and saved in different pixelated formats (e.g. 3 channels x 8 bits= sRGB-24; 4 channels x 8 bits= sRGB-32; 4 channels x 16 bits= sRGB-64).

In operating systems running MS 8 and MAC OS X, it was possible to visualize the difference in the rendered thumbnails, but not in full view mode.

Compression effect was visualized using thumbnail-rendering technique. In normal view, it was not possible for the observer to perceive a difference with the naked eye.

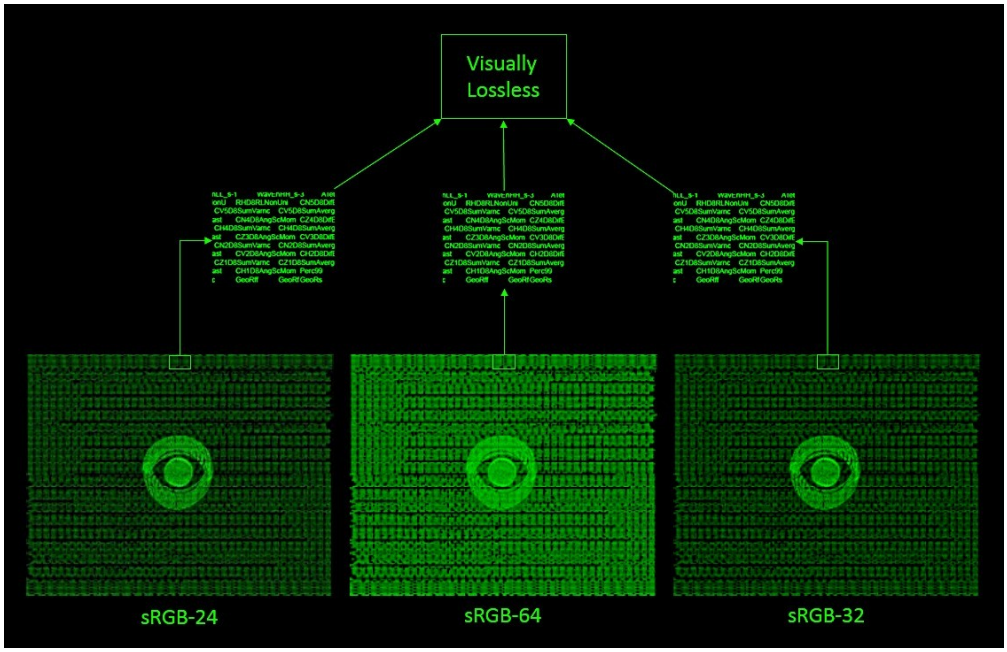

Figure 4: Conversion of vector image to pixel image

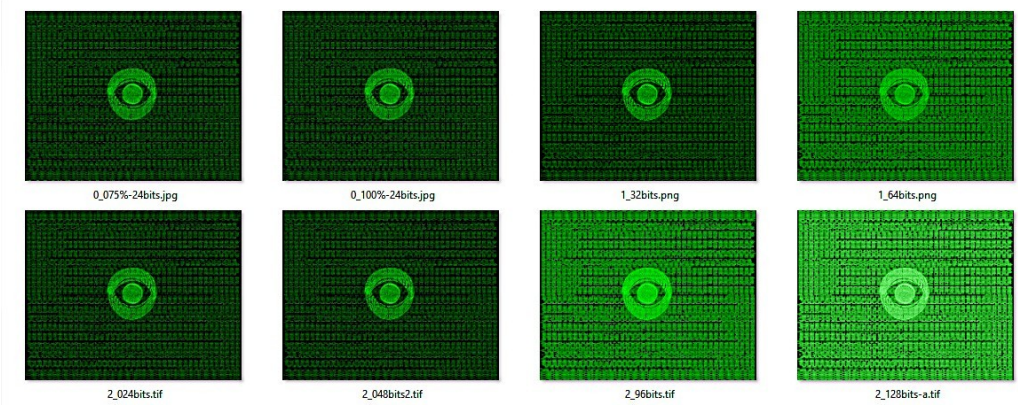

Figure 5: Visualization of image compression

Noise removal was carried out with a plugin in Photoshop. The module setting was as followed: preserve details: 100%; reduce noise: 100%; sharpen details: 0%; strength: 10; remove JPEG artifact: unchecked (this feature is for lossy compression or irreversible compression). 1.5T DICOM files were encoded in 16-bit lossless-JPEG format, while 3T files were natively uncompressed. 1.5T files were decoded to RAW format (sRGB-48) using Photoshop CS6 64- bit Extended. Figure 3 shows how to load RAW files in MaZda. Image dimensions are provided in the names of the files (see appendix for further details). Various compression formats were investigated (figure 5). Then MaZda was used to extract hundreds of parameters from magnetic resonance (MR) images of normal fetal brain. Semi-automatic preprocessing methodologies were used to reduce the parameters and select 13 epitomic parameters. Four ROIs were manually segmented (ventricle, thalamus, grey matter, white matter). Despite the fact that the system was very sensitive to manual input, it was still possible to reproduce the procedures in the trials. We recommend for the operator to have clinical experience with fetal brain MRI and able to correctly identify these anatomical structures.

Observing an image on a radiology monitor in real-time rendering mode is a qualitative method. Hence, extraction of texture features was performed in MaZda to computer various parameters, in order to quantify and confirm a difference between the original image and the denoised image. In this final step, we performed distance-metrics learning classification with artificial neural network (ANN) algorithms implemented in MaZda package. This quantitative process was performed to compare difference between original and denoised MR images, as well as the difference between corresponding original and denoised 3D-mesh images. The parameters were reduced to 13 with ANN algorithms in MaZda. Still and motion media are included in the supplemental data. 3D meshes of each 2D map were generated. It is important to note that we didn't just rely on the 3D appearance. Images were analyzed both qualitatively and quantitatively (table 1, 2, 3, 4; figure 6). The method steps are summarized in figure 2. Rendering 2D images into 3D meshes allowed quick visualization of difference in texture features. Additionally, 3D meshes were re-imported in MaZda for confirmatory comparison and further quantitative analysis.

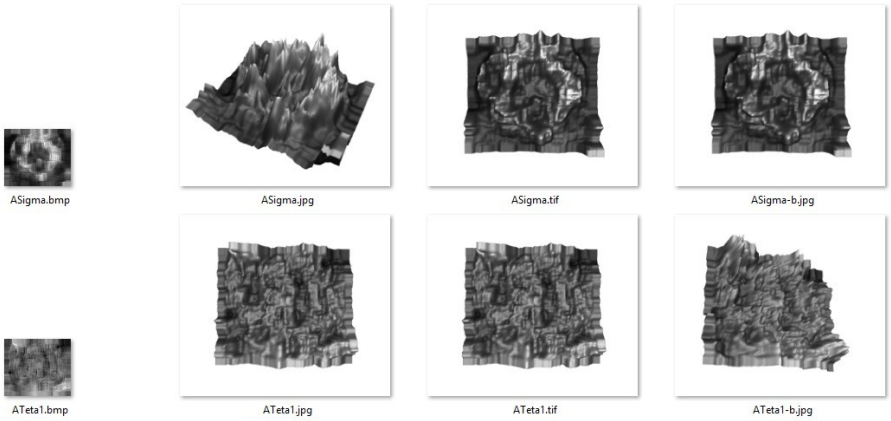

Figure 6: Texture mapping

Each parameter corresponded to a map. TIFF files can be rotated in a 3D viewer (see raw data: DOI: 10.13140/RG.2.1.3252.1842). MaZda effectively and consistently differentiates the original image and from the denoised image. In color space sRGB-48, it was not possible for the unaided-eye observer to differentiate minute noise/artifacts from normal signals (see pre-/post-MR images in the schematic collage presented in figure 1, as well as the original image in the supplemental zip file: subfolders entitled "samples": DOI: 10.13140/RG.2.1.3252.1842). MaZda revealed that both 1.5/3T MRI images were affected by the subtle denoising process (i.e. noise removal with 100% normal signal preservation). 13 epitomic parameters were selected by means of ANN. The outcome depended on the parameter selection. Visualization with 2D motions pictures and 3D-mesh polygons showed the existence of a difference between the images. The data were further processed with quantitative analysis performed in MaZda, using distance- metrics learning classification (raw data: DOI: 10.13140/RG.2.1.3252.1842).

2.3. Advance in knowledge

- This technology enables acquisition and quality control of MR images in HDR formats, as well as epitomic parameterization and classification of CNS structures using applied artificial intelligence.

2.4. Implication for patient care

- The iteration achieved with the texture analysis methodologies presented herein enables the investigation of noise/artifacts in medical images captured with 1.5/3T MRI scanners, as well as differentiation of closely related anatomical structures in prenatal human brain.
- This HCI concept was developed with an intention to complement and improve the performance of obstetricians and radiologists — rather than attempting to artificially replace these trained human readers.
- Abstraction can be utilized to improve accuracy and precision of MRI examinations.

3. Conclusion

In terms of applied artificial intelligence, the visually-lossless phenomenon was an illusion (a deceptive appearance). The epitomic parameters extracted with MaZda revealed that the original samples were affected by subtle denoising. In HDR images (even with visually- lossless compression), it was not possible for the unaided-eye observer to identify a difference, unless artificially rendered. These data could be useful for development of more accurate diagnostic tools to improve interpretation of fetal brain MRI.

4. Constraints, Limitations, and Assumptions

The purpose of this research was to use MaZda 5 RC to extract representative parameters from MRI images. The software could reveal a difference between original and denoised images, while such a difference was undetected by experts. Although no difference between original and denoised images could be observed by naked eyes, we assumed that the information removed by noise removal may actually bear a clinical significance — as yet unknown.

5. Recommendation

Due to the high sensitivity of MaZda, it is recommended to use HDR format to compare the MRI scoring between the original and the denoised image (e.g. uncompressed RAW with 16 bits per channel or higher).

Acknowledgements

The authors gratefully acknowledge prof. Rafal Pawliczak and MUL staff for research coordination, logistics, and administration; prof. Paweł Liberski and MUL neuropathology department for counsels with funds to cover MRI expenses; prof.

Ludomir Stefańczyk and Barlicki hospital staff for sample supply and clinical feedback; prof. Maria Respondek- Liberska and Matki Polki Hospital for sample supply and clinical feedback — as well as prof. Tadeusz Biegański, ICZMP director; prof. Michał Strzelecki and TUL staff for providing MaZda software and technical feedback.

Author Contributions

HG conceived, designed, and carried out the experiment, interpreted the data and drafted the manuscript. Both LS and MRL provided human samples and participated in conceiving/designing the clinical aspects of the research and revising its manuscript. MS provided texture analysis software/plugins and participated in conceiving/designing the technical aspects of the experiment and in revising its manuscript. All authors read and approved the final manuscript.

Competing Interests

The authors declare no financial interests.

References

[1]. Towle, A. (1998). Changes in health care and continuing medical education for the 21st century. BMJ: British Medical Journal, 316(7127), 301.

[2]. Davis, D. A., Thomson, M. A., Oxman, A. D., & Haynes, R. B. (1995). Changing physician performance: a systematic review of the effect of continuing medical education strategies. Jama, 274(9), 700-705.

[3]. Anderson, J. G. (2004). Surgical Training, Error. Jama, 291(14), 1775-1776.

[4]. Scott, J. N., Markert, R. J., & Dunn, M. M. (1998). Critical thinking: change during medical school and relationship to performance in clinical clerkships. Medical education, 32(1), 14-18.

[5]. Brennan, T. A., Sox, C. M., & Burstin, H. R. (1996). Relation between negligent adverse events and the outcomes of medical-malpractice litigation. New England Journal of Medicine, 335(26), 1963-1967.

[6]. Stafford, B. M. (1993). Body criticism: Imaging the unseen in enlightenment art and medicine. mit Press.

[7]. Doi, K. (2006). Diagnostic imaging over the last 50 years: research and development in medical imaging science and technology. Physics in medicine and biology, 51(13), R5.

[8]. Studdert, D. M., Mello, M. M., Sage, W. M., DesRoches, C. M., Peugh, J., Zapert, K., & Brennan, T. A. (2005). Defensive medicine among high-risk specialist physicians in a volatile malpractice environment. Jama, 293(21), 2609-2617.

[9]. Geitung, J. T. (2016). Modern radiology and the use of resources. Too much technology (?)– Not at all. Acta Radiologica, 57(1), 3-5.

[10]. Annapragada, A. (2015). Advances in Nanoparticle Imaging Technology for Vascular Pathologies. Annual review of medicine, 66, 177-193.

[11]. Wood, M. L., Griswold, M. A., Henkelman, M., & Hennig, J. (2015). Inflection Points in Magnetic Resonance Imaging Technology—35 Years of Collaborative Research and Development. Investigative radiology, 50(9), 645-656.

[12]. P. Szczypinski, M. Strzelecki, A Materka, A. Klepaczko, MaZda - A software package for image texture analysis, Computer Methods and Programs in Biomedicine, 94(1), 2009, pp 66-76

[13]. P. Szczypinski, M. Strzelecki, A. Materka, MaZda - a Software for Texture Analysis, Proc. of ISITC 2007, November 23-23, 2007, Republic of Korea, pp. 245-249.

[14]. Weisenfeld, N. I., & Warfield, S. K. (2009). Automatic segmentation of newborn brain MRI. Neuroimage, 47(2), 564-572.

Appendix

Supplemental data are available at DOI: 10.13140/RG.2.1.3252.1842 . The zip file contains three folders:

1) Files for rendered thumbnails: in Windows operating system, a simple way to view rendered image is to open the folder and right click and select view large icon.

2) 1.5T data: it contains 5 subfolders:

- "Samples": RAW files of before-/after- denoising
- "Parameters": 2 report files created with MaZda: one shows all the extracted parameters. The other one shows the parameters used for ANN classification.
- "ORI" = original: 52 files: 13 epitomic parameters x 4 texture maps
- "DSN" = denoised: 52 files: 13 epitomic parameters x 4 texture maps
- "3D-space": still/motion-picture visualization of the difference between the original image and the denoised image.

3) 3T data: it contains the same aforementioned subfolders but with 3T data.

Abbreviations

2D = two-dimensional; 3D = three-dimensional; ANN = artificial neural network; AR = autoregressive model; BMP = bitmap; BMF = byte map font; CAD = computer aided detection or diagnosis (also known as CADe or CADx); CGI = computer generated imaginary; CNS = central nervous system; COM = co-occurrence matrix; COST = European Commission and Cooperation in Science and Technology; DICOM = digital imaging and communications in medicine; HCI = human-computer interaction; HDR = high dynamic range; JPEG = Joint Photographic Experts Group; LCD = liquid crystal display; MAC = Macintosh; MR= magnetic resonance; MRI = magnetic resonance imaging; MS = Microsoft; OS = Operating system; PNG= Portable Network Graphics; RAW = read as written; RC = release candidate (a type of beta version); RLM = run-length matrix; sRGB = red, blue, green (standard color space); sRGB-24 = 8 bits x 3 channels; T = tesla; TIFF = tagged image file format (also known as TIF); TUL = Technical University of Łódź